EPR Spectroscopy

Deutsche Ausgabe: DOI: 10.1002/ange.201504487
Internationale Ausgabe: DOI: 10.1002/anie.201504487

g-Engineering in Hybrid Rotaxanes To Create AB and AB$_2$ Electron Spin Systems: EPR Spectroscopic Studies of Weak Interactions between Dissimilar Electron Spin Qubits

*Antonio Fernandez, Eufemio Moreno Pineda, Christopher A. Muryn, Stephen Sproules, Fabrizio Moro, Grigore A. Timco, Eric J. L. McInnes, and Richard E. P. Winpenny**

Abstract: *Hybrid [2]rotaxanes and pseudorotaxanes are reported where the magnetic interaction between dissimilar spins is controlled to create AB and AB$_2$ electron spin systems, allowing independent control of weakly interacting $S = ^1/_2$ centers.*

Several groups have proposed the idea that molecules could be used as electron spin qubits.[1–6] Molecular qubits can be designed such that phase memory times (T_m) approach other solid-state electron spin technologies,[7] and have the advantage that they can be functionalized by synthetic-chemistry methods. Proposed molecular spin qubits include organic radicals,[2] simple coordination complexes,[7] high-spin[1] and low-spin clusters,[3–5] and 4f ions.[6] One challenge is to bring together ensembles of such qubits, and particularly to bring together qubits with different electronic *g*-factors, so called *g*-engineering,[2,6] which would allow the qubits to be addressed individually and controllably within a complex molecule. Takui and co-workers have done this using elegant organic chemistry, and have reported the operation of the CNOT gate using such an approach.[2] Herein we show how similar *g*-engineering can be achieved using coordination chemistry of 3d metal cages.

We have been studying heterometallic {Cr$_7$M} rings for their fascinating spin physics.[8] Where M is Ni, antiferromagnetic exchange coupling gives a well-isolated $S = ^1/_2$ ground state; pulsed electron paramagnetic resonance (EPR) spectroscopy shows these have sufficiently long phase memory times to use as qubits.[9] The chemical robustness and versatility of these units allow their incorporation in hybrid [2]rotaxanes.[10] Herein we use a thread, PyCH$_2$NHCH$_2$CH$_2$Ph, that features a pyridyl group as a stopper on one end and a benzyl group as stopper at the other end, to make the [2]rotaxane [PyCH$_2$NH$_2$CH$_2$CH$_2$Ph]-[Cr$_7$Ni(μ-F)$_8$(O$_2$C*t*Bu)$_{16}$] **1** in 32 % yield (see the Supporting Information).

The stoichiometric reaction of **1** with [Cu(hfac)$_2$] (Hhfac = 1,1,1,6,6,6-hexafluoroacetylacetone) yields another [2]rotaxane {[Cu(hfac)$_2$][PyCH$_2$NH$_2$CH$_2$CH$_2$Ph][Cr$_7$Ni(μ-F)$_8$(O$_2$C*t*Bu)$_{16}$]} **2**. X-ray crystallography[11] of **2** confirms that [Cu(hfac)$_2$] has bound to the pyridyl of the rotaxane thread (Figure 1 a,b and Figure S1 in the Supporting Information).

The heterometallic ring in **2** is unchanged from that in rotaxane **1**, containing eight metals in an octagon, bridged by fluoride and pivalate ligands (Figure 1 b). The ammonium group of the thread hydrogen bonds to the fluorides within the metal octagon. The pyridyl group from the thread binds to copper, occupying the apical site of a square-based pyramid.

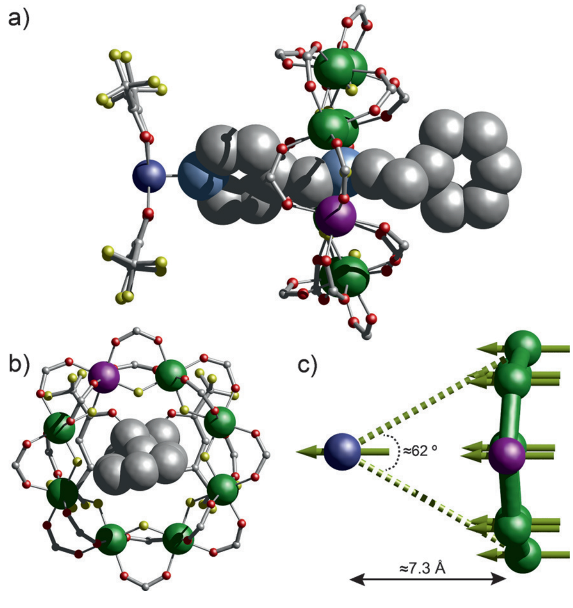

Figure 1. Crystal structure of **2** (ball-and-stick model) viewed a) side-on, and b) perpendicular to the {Cr$_7$Ni} plane. c) Arrow representation of the g_z-component of the Cu^{II} and {Cr$_7$Ni} fragments. The dotted lines are Cu···M vectors for opposite M sites on the {Cr$_7$Ni} ring and the average *trans* M–Cu–M angle is shown. Atom colors: Cr = green, Ni = purple, Cu = dark blue, F = yellow, O = red, C = gray, N = pale blue. H atoms and *t*Bu groups of pivalate ligands have been omitted for clarity. C and N atoms of the thread are drawn larger to highlight this structural feature.

---

[*] Dr. A. Fernandez, Dr. E. Moreno Pineda,[+] Dr. C. A. Muryn, Dr. S. Sproules,[++] Dr. F. Moro,[+++] Dr. G. A. Timco, Prof. E. J. L. McInnes, Prof. R. E. P. Winpenny
School of Chemistry, The University of Manchester
Oxford Road, Manchester M13 9PL (UK)
E-mail: Richard.winpenny@manchester.ac.uk

[+] Current address: Institute of Nanotechnology
Karlsruhe Institute of Technology
76344 Eggenstein-Leopoldshafen (Germany)

[++] Current address: WestCHEM, School of Chemistry
University of Glasgow, Glasgow G12 8QQ (UK)

[+++] Current address: School of Physics and Astronomy
The University of Nottingham
University Park, NG7 2RD, Nottingham (UK)

Supporting information for this article is available on the WWW under http://dx.doi.org/10.1002/anie.201504487.

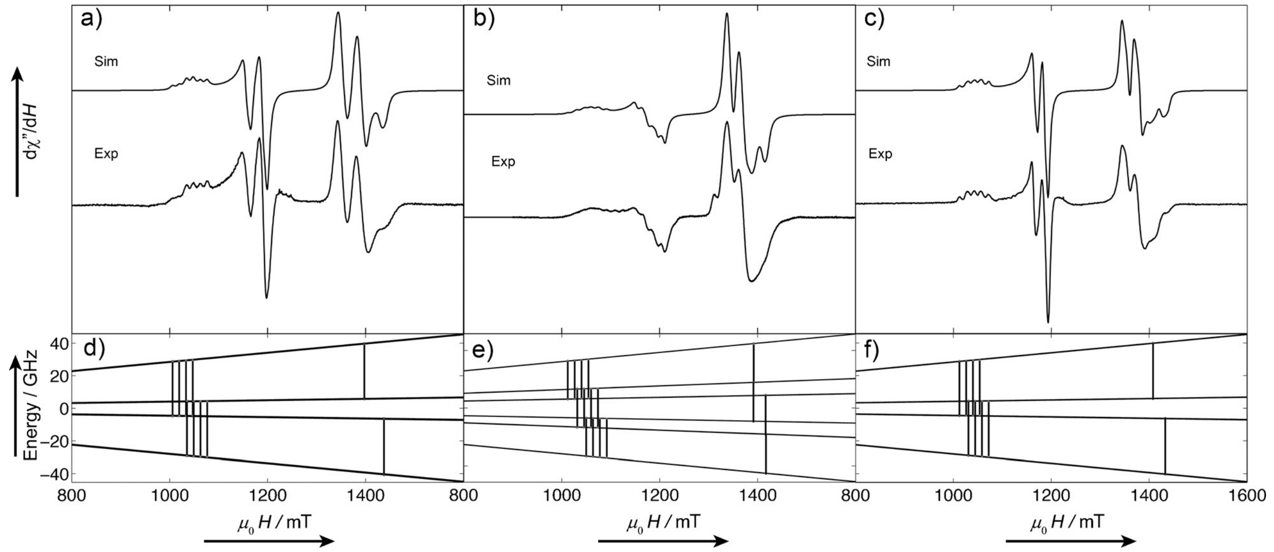

Figure 2. Experimental Q-band (ca. 34 GHz) EPR spectra and simulations for a) **2**, b) **3**, and c) **5** in a 1:1 solution of toluene/CH_2Cl_2 at 5 K. Simulation parameters: a) $g_{x,y,z}^{Cr_7Ni} = 1.780, 1.765, 1.710$; $g_{x,y,z}^{Cu} = 2.065, 2.045, 2.325$; $A_z^{Cu} = 450$ MHz; $J = -0.032\ cm^{-1}$; b) $g_{x,y,z}^{Cr_7Ni} = 1.785, 1.775, 1.715$; $g_{x,y,z}^{Cu} = 2.050, 2.020, 2.287$; $A_z^{Cu} = 450$ MHz; $J = -0.020\ cm^{-1}$; and c) $g_{x,y,z}^{Cr_7Ni} = 1.780, 1.775, 1.705$; $g_{x,y,z}^{Cu} = 2.060, 2.045, 2.322$; $A_z^{Cu} = 450$ MHz; $J = -0.020\ cm^{-1}$. d–f) Zeeman plots for *H* along the molecular *z* axis, with Q-band EPR transitions shown.

The distance between the centroid of the {Cr_7Ni} ring and the Cu^{II} center is 7.332(1) Å, whereas the average Cu···Cr/Ni distance is 8.56 Å with the Cr···Cu vectors making an average angle (θ) of 31° to the {Cr_7Ni} normal (which is parallel to the Cu−N vector, Figure 1 c). The pivalate moieties in the ring are sterically demanding and there is little flexibility in the molecule (Figure S1); therefore the crystal structure of **2** is representative of the structure in solution.

The only through-bond pathway between the spin centers of the {Cr_7Ni} ring and the single Cu^{II} site involves hydrogen bonds between fluorides and the protonated ammonium site of the thread, therefore any magnetic interactions between the two components are expected to be very weak. Nevertheless, clear evidence of such interactions is detected by continuous wave (cw) EPR spectroscopy (Figure 2).

At low temperature (5 K) only the $S = {}^1\!/_2$ ground state of {Cr_7Ni} is populated substantially; this state is approximately axially symmetric with $g_{\perp}^{Cr_7Ni} \approx 1.78$ and $g_{\parallel}^{Cr_7Ni} \approx 1.74$ where the "unique" axis is perpendicular to the {Cr_7Ni} plane.[12] The EPR spectrum of **2** at Q-band (34 GHz) and 5 K is very simple with two sets of features, centered at the *g*-values expected for {Cr_7Ni} and for Cu^{II} ($g_{\perp}^{Cu} \approx 2.05$, $g_{\parallel}^{Cu} \approx 2.30$) with resolution of copper hyperfine coupling (A^{Cu}) on the $g_{\parallel}^{Cu}$ feature. Each of these *g*-features is split into a spectroscopic doublet; that is, the spectrum has the form of a simple AB spin pattern, where the spin–spin coupling is much smaller than the difference in Zeeman energy (the difference in Zeeman energy is 0.17 cm^{-1} for a static field of 1.21 T and $g = 2.1$ and 1.8). This scenario is familiar from NMR spectroscopy, but examples of AB electron spin patterns resolved by cw-EPR spectroscopy are rare.[2a,13]

The resolution of the spectrum is such that we can read the parallel and perpendicular components of the interaction (J) between the Cu and {Cr_7Ni} sites directly from the spectrum. As a result of the fact that the local z axis at the Cu site (along the Cu−N vector) is parallel to the normal of the {Cr_7Ni} ring, the $g_{\parallel}^{Cu}$ and $g_{\parallel}^{Cr_7Ni}$ axes correspond to the same molecular orientation of **2**. The multiplet pattern on the $g_{\parallel}^{Cu}$ signal clearly shows two overlapping hyperfine quartets ($^{63}Cu^{II}$, $^{65}Cu^{II}$, $I = {}^3\!/_2$), thus the $J_{\parallel}$ value is of the same order as the $A_{\parallel}^{Cu}$ value. Measurement of the doublet splittings of the $g_{\perp}$ features then reveals that $J_{\perp} \approx J_{\parallel}$, that is, the interaction is essentially isotropic. To test this we simulated[14] the spectrum with a simple isotropic exchange Hamiltonian:

$$\hat{H} = \mu_B \hat{S}^{Cu} \cdot \mathbf{g}^{Cu} \cdot \vec{B} + \mu_B \hat{S}^{Cr_7Ni} \cdot \mathbf{g}^{Cr_7Ni} \cdot \vec{B} + \hat{S}^{Cu} \cdot \mathbf{A}^{Cu} \cdot \hat{I}^{Cu} - J \hat{S}^{Cu} \cdot \hat{S}^{Cr_7Ni}$$

We initially fixed the *g*-values and Cu^{II} hyperfine interaction from model complexes, with J as the only free variable, but then refined all parameters: better fits are found by introducing a slight rhombicity in the *g*-value (Figure 2 a). This gives $J = -0.032\ cm^{-1}$; the relative transition intensities within the exchange doublets are sensitive to the sign of the J value.

The interaction is weak and antiferromagnetic, but it is perhaps surprising it is seen at all as the only through-bond pathway involves hydrogen bonds. As the interaction is isotropic this implies that it cannot be dipolar (through space) in origin. For comparison, we have calculated the dipolar interaction (D) for **2**. A very crude treatment is to take {Cr_7Ni} as a spin localized at its centroid: this gives $D_{xx,yy} = +0.004$, $D_{zz} = -0.009\ cm^{-1}$. This is too weak to explain the spectrum and moreover such a model cannot, by definition, give an isotropic interaction. A more rigorous treatment is to calculate the full dipolar interaction matrix **D** for the nine-spin system: the effective {Cr_7Ni}···Cu interaction can be calculated by the sum of the individual Cr···Cu and Ni···Cu dipolar interactions weighted by the projection factors of the Cr^{III} and Ni^{II} local spins onto the $S = {}^1\!/_2$ ground state of the {Cr_7Ni} ring (see the Supporting Information).[16] We used spin projection factors determined from solid-state ^{53}Cr NMR spectroscopic studies on $(Me_2NH_2)[Cr_7NiF_8(O_2CtBu)_{16}]$.[17] The full calculated dipolar matrix is given in the Supporting Information. The leading term of the dipolar matrix (orientated along the $g_{\|}$ direction) is $D_{zz} = -0.0034\ \text{cm}^{-1}$, that is, an order of magnitude smaller than the experimentally measured coupling. Including this **D** matrix makes no significant difference to the calculated EPR spectrum. Thus, the ring⋯Cu couplings are not a result of dipolar interactions. The pathway for the isotropic exchange interaction remains unclear but must be through bond. Interestingly, the value found here falls within the range predicted by Coffman and Buettner's[15] empirical limit function for long-range superexchange interactions. In the cases they discuss there are always more obvious through bond pathways.

This result led us to explore closely related but more complex heterospin systems. First, $[Cu(NO_3)_2(Me_2CO)]\text{-}\{[PyCH_2NH_2CH_2CH_2Et][Cr_7Ni(\mu\text{-}F)_8(O_2CtBu)_{16}]\}_2$ **3** was synthesized, which contains two pseudo[2]rotaxanes bound to a single Cu^{II} site (Figure 3 a). The thread in **3** differs from that in **1** and **2**, with an ethyl group at one end rather than a benzyl, which could in principle allow dethreading in solution. However, this process is not detected, as demonstrated from the form of its EPR spectrum. The Cu^{II} site has the two pyridyl rings from the pseudorotaxanes *trans* to each other, with two nitrates and an acetone coordinated in the plane. The nitrates are chelating with one long (2.6 Å) and one short (1.95 Å) Cu−O distance each. The two Cu−N and the two short Cu−O(nitrate) distances define a square plane (N-Cu-N and O-Cu-O 168 and 175°, respectively) with the acetone in an axial position (Cu−O 2.41 Å). Thus the best description of the Cu^{II} geometry seems to be again square pyramidal, but now with the axial orientation perpendicular to the $\{Cr_7Ni\}$ planes. As with **2**, the steric requirements of the pivalate ligands lead to the structure of **3** being rigid in solution (Figure S2).

Second, to increase the complexity further, a [3]rotaxane was made about an axle with a pyridyl at each end: $[\{PyCH_2NH_2(CH_2)_5\}_2][Cr_7Ni(\mu\text{-}F)_8(O_2CtBu)_{16}]_2]$ **4**.[18] Coordination of a $[Cu(hfac)_2]$ unit to each end of **4** then gives the system $[Cu(hfac)_2(H_2O)]_2[\{PyCH_2NH_2(CH_2)_5\}_2][Cr_7Ni(\mu\text{-}F)_8\text{-}(O_2CtBu)_{16}]_2]$ **5** (Figure 3 b). The copper coordination geometry is now six-coordinate with two hfac ligands and a water molecule, with the water molecule coordinated *cis* to the pyridyl ring. The Cu−O/N distances are surprisingly regular (Cu−N 2.21, Cu−O 2.126–2.162 Å). Thus it is unclear where the unique Cu^{II} axis is located. The relationship between the $\{Cr_7Ni\}$ rings and Cu^{II} ions in both **3** and **5** are similar to that in **2**, because in each case the ring is formed around the ammonium site of R-$NH_2CH_2CH_2$-pyridyl where the pyridyl binds to the Cu^{II} center (**3**: $\{Cr_7Ni\}$ centroid⋯Cu 7.34 and 7.07 Å, average Cr⋯Cu 8.44 Å, average $\theta = 31°$; **5**: $\{Cr_7Ni\}$ centroid⋯Cu 7.34 Å;, average Cr⋯Cu 8.54 Å, average $\theta = 31°$). Unlike in **2** and **3**, there is flexibility in **5** (Figure S3) because of the C_5 chain at the center of the [3]rotaxane.

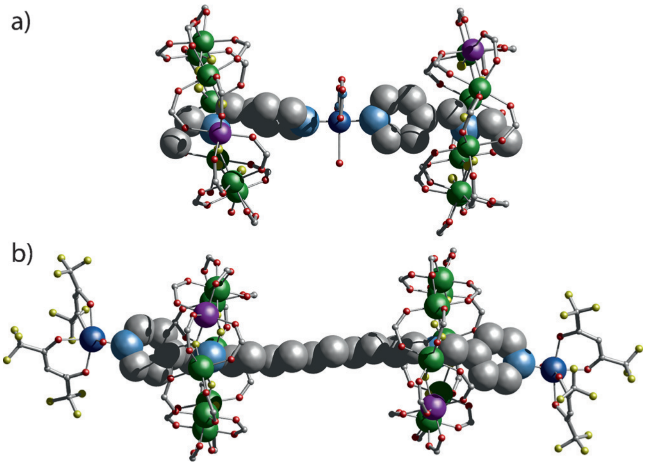

Figure 3. Side-view crystal structure (ball-and-stick model) of a) pseudo[2]rotaxanes **3** and b) [3]rotaxane **5**. Atom colors: Cr = green, Ni = purple, Cu = dark blue, F = yellow, O = red, C = gray, N = pale blue. H atoms and *t*Bu groups of pivalate ligands have been omitted for clarity.

For both **3** and **5** the Q-band EPR spectra of frozen solutions at 5 K again show weak coupling. For **3** an AB_2 spin system pattern is obtained, with the resonance signals attributable to the $\{Cr_7Ni\}$ ring (the B spin) split into a doublet, whereas the resonances for the Cu center (the A spin) are split into 1:2:1 triplets (Figure 2 b). The spectrum of **4** is very similar to that of **1**, that is, that of an isolated $\{Cr_7Ni\}$ ring, where any $\{Cr_7Ni\}\cdots\{Cr_7Ni\}$ interaction within the [3]rotaxane is very weak and not detectable by cw-EPR. This may be connected to the flexibility of the thread resulting from the saturated C_5 chain at the center. The spectrum of **5** is very similar to that of **2** with a weak $\{Cr_7Ni\}\cdots$Cu interaction; the spin structure (as regards cw-EPR) is therefore two very weakly or non-interacting AB spin pairs (Figure 2 c). Simulations of **3** and **5** both give $J = -0.020\ \text{cm}^{-1}$ (Figure 2 b,c). Although the relationship between the $\{Cr_7Ni\}$ and Cu^{II} fragments are similar in each case, minor changes in the spin coupling are justified because of the differing coordination geometry at the Cu^{II} center. In **2** the "unique" (z) axis of the Cu^{II} ion (defining the orientation of the $d_{x^2-y^2}$ magnetic orbital) is unambiguously parallel to the $\{Cr_7Ni\}\cdots$Cu axis (or equivalently the Cu−N direction). In **3**, this axis is orthogonal to $\{Cr_7Ni\}\cdots$Cu; the situation in **5** is ambiguous.

The weak coupling regime of AB spin systems allows the spins to be addressed individually. This is the basis of the g-engineering approach of Takui and co-workers to construct a CNOT gate with dissimilar organic radicals,[2] and towards Lloyd's proposal of periodic $(ABC)_n$ arrays using inequivalently orientated metal ions in helicates.[19] The heterospin structure of **2**, and its dimerization into a more complex array in **5**, shows how such arrays can be achieved exploiting the facile coupling between molecules enabled by coordination and supramolecular-chemistry approaches.

An important question is whether such complex systems can be constructed without deleterious effects on the spin coherence properties of the components. To test this we measured the phase memory times (T_m) for **2** and **5** by pulsed EPR at the X-band using a standard Hahn echo sequence [$\pi/2$-τ-π-τ-echo].

Static magnetic-field positions were chosen that selectively pumped EPR transitions on the $\{Cr_7Ni\}$ ring and on the

Cu^{II} site (409 and 310 mT, respectively, for **2**; Figure S4). The T_m value for the $\{Cr_7Ni\}$ component is circa 600 ns at 5 K in both **2** and **5** (Figure S5). This is in the 400–700 ns range (depending on the nature of the R substituent) found for isolated $[R_2NH_2][Cr_7Ni(\mu\text{-}F)_8(O_2CtBu)_{16}]$ at 5 K.[9] T_m times for the Cu^{II} resonance are larger, at 1.0 μs for both **2** and **5**, and of the same order as found for related isolated Cu^{II} complexes, for example, $[Cu(hfac)_2(4,4'\text{-}Me_2\text{-}bipy)]$ has $T_m =$ 3 μs at 5 K.[20] Thus, the phase memory times are not significantly decreased as a result of the interspin interaction. This bodes well for performing spin manipulation experiments in supramolecular arrays of molecular nanomagnets.

The next steps require tuning the interaction strengths and Zeeman frequencies such that the components can be addressed individually within the resonator bandwidths available with current pulsed microwave technologies. The interaction strength will be controllable through supramolecular chemistry. The difference in Zeeman frequency could be achieved, for example, with spin clusters of marginally different *g*-values[21] or with homospin clusters exploiting non-parallel orientations and *g*-anisotropy.[22]

Acknowledgements

This work was supported by the EPSRC (UK, EP/L018470/1), the National EPR Facility, and the European Commission (Marie Curie Intra-European Fellowship to A.F. (300402)). E.M.P. thanks the Panamanian agency SENACYT-IFARHU for funding. We also thank the EPSRC (UK) for funding an X-ray diffractometer (grant number EP/K039547/1).

Keywords: EPR spectroscopy · heterometallic complexes · magnetic properties · quantum computing · rotaxanes

How to cite: *Angew. Chem. Int. Ed.* **2015**, *54*, 10858–10861
Angew. Chem. **2015**, *127*, 11008–11011

---

[1] M. Leuenberger, D. Loss, *Nature* **2001**, *410*, 789.

[2] a) S. Nakazawa, S. Nishida, T. Ise, T. Yoshino, N. R. Mori, D. Rahimi, K. Sato, Y. Morita, K. Toyota, D. Shiomi, M. Kitagawa, H. Hara, P. Carl, P. Höfer, T. Takui, *Angew. Chem. Int. Ed.* **2012**, *51*, 9860; *Angew. Chem.* **2012**, *124*, 9998; b) K. Sato, S. Nakazawa, R. Rahimi, T. Ise, S. Nishida, T. Yoshino, N. Mori, K. Toyota, D. Shiomi, Y. Yakiyama, Y. Morita, M. Kitagawa, K. Nakasuji, M. Nakahara, H. Hara, P. Carl, P. Höfer, T. Takui, *J. Mater. Chem.* **2009**, *19*, 3739.

[3] F. Meier, J. Levy, D. Loss, *Phys. Rev. Lett.* **2003**, *90*, 47901.

[4] F. Troiani, A. Ghirri, M. Affronte, S. Carretta, P. Santini, G. Amoretti, S. Piligkos, G. Timco, R. E. P. Winpenny, *Phys. Rev. Lett.* **2005**, *94*, 207208.

[5] J. Lehmann, A. Gaita-Ariño, E. Coronado, D. Loss, *Nat. Nanotechnol.* **2007**, *2*, 312.

[6] D. Aguilà, L. A. Barrios, V. Velasco, O. Roubeau, A. Repollés, P. J. Alonso, J. Sesé, S. J. Teat, F. Luis, G. Aromí, *J. Am. Chem. Soc.* **2014**, *136*, 14215.

[7] a) K. Bader, D. Dengler, S. Lenz, B. Endeward, S.-D. Jiang, P. Neugebauer, J. v. Slageren, *Nat. Commun.* **2014**, *5*, DOI: 10.1038/ncomms6304; b) M. Warner, S. Din, I. S. Tupitsyn, G. W. Morley, A. Stoneham, J. A. Gardener, Z. Wu, A. J. Fisher, S. Heutz, C. W. M. Kay, G. Aeppli, *Nature* **2013**, *503*, 504; c) M. J. Graham, J. M. Zadrozny, M. Shiddiq, J. S. Anderson, M. S. Fataftah, S. Hill, D. E. Freedman, *J. Am. Chem. Soc.* **2014**, *136*, 7623.

[8] a) M. Affronte, S. Carretta, G. A. Timco, R. E. P. Winpenny, *Chem. Commun.* **2007**, 1789; b) G. A. Timco, E. J. L. McInnes, R. E. P. Winpenny, *Chem. Soc. Rev.* **2013**, *42*, 1796.

[9] a) A. Ardavan, O. Rival, J. J. L. Morton, S. J. Blundell, A. M. Tyryshkin, G. A. Timco, R. E. P. Winpenny, *Phys. Rev. Lett.* **2007**, *98*, 057201; b) C. J. Wedge, R. E. George, G. A. Timco, F. Tuna, S. Rigby, E. J. L. McInnes, R. E. P. Winpenny, S. J. Blundell, A. Ardavan, *Phys. Rev. Lett.* **2012**, *108*, 107204.

[10] a) C.-F. Lee, D. A. Leigh, R. G. Pritchard, D. Schultz, S. J. Teat, G. A. Timco, R. E. P. Winpenny, *Nature* **2009**, *458*, 314; b) B. Ballesteros, T. B. Faust, C.-F. Lee, D. A. Leigh, C. A. Muryn, R. G. Pritchard, D. Schultz, S. J. Teat, G. A. Timco, R. E. P. Winpenny, *J. Am. Chem. Soc.* **2010**, *132*, 15435.

[11] a) Crystal data for **2** $[C_{104}H_{163}Cr_7CuF_{20}N_2O_{36}Ni]$: $M_r = 2883.61$, orthorhombic, space group *Pnaa*, $T = 100.15$ K, $a = 20.2386(7)$, $b = 27.6927(6)$, $c = 27.4034(9)$ Å, $V = 15358.6(8)$ Å^3, $Z = 4$, $\rho = 1.247\ g\,cm^{-3}$, total data = 13572, $R_1 = 0.1238$ for $I \geq 2\sigma\ (I)$ and $wR_2 = 0.3326$. Crystal data for **3** $[C_{179}H_{320}Cr_{14}CuF_{16}N_6Ni_2O_{71}]$: $M_r = 4905.35$, orthorhombic, space group $Pna2_1$, $T = 150.15$ K, $a = 51.6574(10)$, $b = 27.1191(6)$, $c = 20.0038(3)$ Å, $V = 28023.4(9)$ Å^3, $Z = 4$, $\rho = 1.163\ g\,cm^{-3}$, total data = 36449, $R_1 = 0.0993$ for $I \geq 2\sigma\ (I)$ and $wR_2 = 0.2468$. CCDC 1401242 (**2**), 1401243 (**3**), and 916469 (**5**) contain the supplementary crystallographic data for this paper. These data can be obtained free of charge from The Cambridge Crystallographic Data Centre. Crystallographic data for **2** was collected on a Bruker Prospector CCD diffractometer with CuKα radiation ($\lambda = 1.5418$ Å). Crystallographic data for **3** was collected on an Agilent SuperNova CCD diffractometer with MoKα radiation ($\lambda = 0.71073$ Å) and was solved using SHELX; b) G. M. Sheldrick, *Acta Crystallogr. Sect. A* **2008**, *64*, 112.

[12] S. Piligkos, H. Weihe, E. Bill, F. Neese, H. El Mkami, G. M. Smith, D. Collison, G. Rajaraman, G. A. Timco, R. E. P. Winpenny, E. J. L. McInnes, *Chem. Eur. J.* **2009**, *15*, 3152.

[13] G. R. Eaton, S. S. Eaton, *Acc. Chem. Res.* **1998**, *31*, 107.

[14] Using *EasySpin*: S. Stoll, A. Schweiger, *J. Magn. Reson.* **2006**, *178*, 42.

[15] R. E. Coffman, G. R. Buettner, *J. Phys. Chem.* **1979**, *83*, 2387.

[16] C. Elsässer, M. Brecht, R. Bittl, *J. Am. Chem. Soc.* **2002**, *124*, 12606.

[17] C. M. Casadei, L. Bordonali, Y. Furukawa, F. Borsa, E. Garlatti, A. Lascialfari, S. Carretta, S. Sanna, G. Timco, R. E. P. Winpenny, *J. Phys. Condens. Matter* **2012**, *24*, 406002.

[18] G. F. S. Whitehead, B. Cross, L. Carthy, V. A. Milway, H. Rath, A. Fernandez, S. L. Heath, C. A. Muryn, R. G. Pritchard, S. J. Teat, G. A. Timco, R. E. P. Winpenny, *Chem. Commun.* **2013**, *49*, 7195.

[19] a) S. Lloyd, *Science* **1993**, *261*, 1569; b) Y. Morita, Y. Yakiyama, S. Nakazawa, T. Murata, T. Ise, D. Hashizume, D. Shiomi, K. Sato, M. Kitagawa, K. Nakasuji, T. Takui, *J. Am. Chem. Soc.* **2010**, *132*, 6944.

[20] J. M. Burchfield, J.-L. Du, K. M. More, S. S. Eaton, G. R. Eaton, *Inorg. Chim. Acta* **1997**, *263*, 23.

[21] G. A. Timco, E. J. L. McInnes, R. G. Pritchard, F. Tuna, R. E. P. Winpenny, *Angew. Chem. Int. Ed.* **2008**, *47*, 9681; *Angew. Chem.* **2008**, *120*, 9827.

[22] T. B. Faust, V. Bellini, A. Candini, S. Carretta, L. Carthy, D. Collison, R. J. Docherty, J. Kenyon, G. Lorusso, J. Machin, E. J. L. McInnes, C. A. Muryn, R. G. Pritchard, S. J. Teat, G. A. Timco, F. Tuna, G. F. S. Whitehead, W. Wernsdorfer, M. Affronte, R. E. P. Winpenny, *Chem. Eur. J.* **2011**, *17*, 14020.

Received: May 18, 2015